The cytochrome **bc$_1$** *complex as an antipathogenic target*

Nicholas Fisher[1], Brigitte Meunier[2] and Giancarlo A. Biagini[3]*

[1] MSU-DOE Plant Research Laboratory, Michigan State University, East Lansing, MI 48824, USA

[2] Université Paris-Saclay, CEA, CNRS, Institute for Integrative Biology of the Cell (I2BC), 91198, Gif-sur-Yvette, France

[3] Research Centre for Drugs & Diagnostics, Parasitology Department, Liverpool School of Tropical Medicine, Liverpool, L3 5QA, UK

*Correspondence: nefisher@msu.edu ; Tel: +1 517-432-0071; MSU-DOE Plant Research Laboratory, 612 Wilson Rd., Michigan State University, East Lansing, Michigan 48824, USA.

Abstract

The cytochrome bc_1 complex is a key component of the mitochondrial respiratory chains of many eukaryotic microorganisms that are pathogenic for plants or humans, such as fungi responsible for crop diseases and *Plasmodium falciparum*, which causes human malaria. Cytochrome bc_1 is an enzyme that contains two (ubi)quinone/quinol binding sites, which can be exploited for the development of fungicidal and chemotherapeutic agents. Here we review recent progress in determination of the structure and mechanism of action of cytochrome bc_1, and the associated development of antimicrobial agents (and associated resistance mechanisms) targeting its activity.

Keywords

Cytochrome bc_1; Electron transport; Fungicide; G143A; Malaria; QoI/QiI; Resistance

Abbreviations

Δp - protonmotive force

AOX - (mitochondrial) alternative oxidase

cyt - cytochrome

DHODH - dihydroorotate dehydrogenase

$E_{m,7}$ - (redox) midpoint potential at pH 7

ED - extrinsic domain

EPR - electron paramagnetic resonance

FRAC - Fungicide Resistance Action Committee

HHDBT - *n*-heptyl-6-hydroxy-4,7-dioxobenzothiazole

IMM - inner mitochondrial membrane

IMS - (mitochondrial) intermembrane space

41 ISP - (Rieske) iron-sulphur protein

42 NQNO - *n*-nonyl quinoline N-oxide

43 MDR - multiple drug resistance

44 MOA - methoxyacrylate

45 mtDNA - mitochondrial DNA

46 Q_i - site of (ubi)quinone reduction within cytochrome *b*

47 QiI - Q_i site inhibitor

48 Q_o - site of (ubi)quinol oxidation within cytochrome *b*

49 QoI - Q_o site inhibitor

50 ROS - reactive oxygen species

51 SAR - structure activity relationship

52 SHAM - salicylhydroxamic acid

53 SQ_i - semiquinone bound at the Q_i site of cytochrome *b*

54 SQ_o - semiquinone bound at the Qo site of cytochrome *b*

55 UHDBT - *n*-undecyl hydroxy dibenzothiazole

56

Introduction and general enzymatic mechanism of the cytochrome bc_1 complex

The cytochrome bc_1 complex (respiratory Complex III, Cyt bc_1, EC: 1.10.2.2) of eukaryotic mitochondrial- and prokaryotic energy transducing membranes is a proven target for antimicrobial agents of medical and agricultural interest [1-7]. This enzyme, which is widespread in nature, functions as a protonmotive ubiquinol:cytochrome *c* oxidoreductase, conserving- and converting the Gibbs energy obtained from the exergonic oxidation of ubiquinol by cytochrome *c* into a transmembrane proton gradient which may be harnessed for other endergonic processes, typically ATP synthesis by an F_oF_1 ATP synthase [8-9] .

Cyt bc_1 is a multimeric, homodimeric complex. In eukaroytes (the focus of this review), the monomer consists of 10-11 discrete polypeptides, with a molecular mass of approximately 240 kDa [8,10]. All subunits are nuclearly encoded with the exception of cytochrome *b* (cyt *b*), which is encoded by the mitochondrial genome. Three subunits - cyt *b*, the Rieske [2Fe2S] iron-sulphur protein (ISP) and cytochrome c_1 (cyt c_1) form the highly conserved electron- and proton transferring catalytic engine of the enzyme (Fig. 1), embedded within the inner mitochondrial membrane (IMM). The [2Fe2S] cluster and haem group of cyt c_1 form the 'high potential' chain of cyt bc_1, with midpoint redox potentials ($E_{m,7}$) of approximately +280 and +240 mV respectively. The cytochrome *b* polypeptide forms the 'low potential' transmembrane electron transfer pathway and binds two b-type haems, designated b_L and b_H, with $E_{m,7}$ values of approximately -100 and +50 mV respectively. (For reference, the $E_{m,7}$ for the *2 electron* redox chemistry of the ubiquinone/ubiquinol redox couple is approximately + 60 mV). During the catalytic cycle, which is described in more detail below, cyt bc_1 oxidises two molecules of ubiquinol in a stepwise manner, reducing two molecules of the soluble acceptor cytochrome *c* and one molecule of ubiquinone. The protonmotive activity inherent to this catalytic cycle results in the deposition of four protons against the electrochemical gradient into the intermembrane space, per two electrons transferred to cyt *c*, with the concomitant uptake of two protons from the mitochondrial matrix [9,11,12].

The ubiquinol- and ubiquinone binding sites of cyt bc_1 are termed Q_o and Q_i, for the sites of (ubi)quinol oxidation and (ubi)quinone reduction, respectively. They form exploitable targets for competitive inhibitors and are located within cyt *b*, disposed on opposite sides of the IMM and linked by haems b_L and b_H. The bifurcating electron-transfer chemistry between the high- and low

potential chains of cyt bc_1 is highly unusual, and best understood through the framework of the Q-cycle model (Fig. 2), originally proposed by Peter Mitchell in 1975 and substantially developed by others since [13-18]. The basic tenets of the model are this. A ubiquinol molecule binds at the quinol oxidation (Q_o) site of cyt *b*, located towards the intermembrane space (i.e. electrochemically positive)-side of the IMM. This ubiquinol serves as a one-electron reductant for the [2Fe2S] cluster of the mobile extrinsic domain of the ISP (the ISP-ED), the entry point for the high potential chain within bc_1. The ISP-ED effectively acts as a tethered substrate and kinetic gate facilitating electron bifurcation, although it is important to note that this in itself is not the only factor controlling the bifurcation reaction [19-22]. This electron transfer reaction from ubiquinol to the ISP-ED (which is rate-limiting for the chemistry at Q_o) generates a strongly-reducing semiquinone (SQ_o) radical at Q_o. The reactivity of SQ_o must be carefully controlled to minimise energetically wasteful (and potentially harmful) side reactions with molecular oxygen. The mechanisms by which this radical intermediate - an elusive species - is managed at Q_o are subject to much investigation, discussion of which is beyond the scope of this review, but the interested reader is referred to [23-26] for further details. Protons released from ubiquinol oxidation at Q_o are deposited into the intermembrane space (IMS) bulk phase. SQ_o is of sufficiently negative redox potential (c. -160 mV) to reduce the low potential chain within cyt *b*, with electron entry at haem b_L, which is then rapidly oxidised by haem b_H, the electron donor to Q_i-bound ubiquinone. This one electron transfer reaction creates a tightly bound (and relatively stable) semiquinone species at Q_i (SQ_i), which is reduced to ubiquinol by a second turnover of the Q_o site and uptake of two protons from the mitochondrial matrix, and the cycle is complete. The tight binding of SQ_i at Q_i ensures that the thermodynamics are favourable for the first one-electron transfer reaction to substrate ubiquinone at this site, which otherwise would be energetically uphill [9].

Structure, function and inhibition of the cyt bc_1 Q_o- and Q_i sites

High resolution (< 3.0 Å) atomic structures of cyt bc_1 co-crystallised with a variety of Q_o/Q_i site occupants are available for the chicken, bovine, yeast (*Saccharomyces cerevisiae*) and bacterial (*Rhodobacter sphaeroides*, *R. capsulatus* and *Paracoccus denitrificans*) enzymes (see survey in [10]). Recently, single particle cryo-electron microscopy has proven to be useful tool for structural investigation of this enzyme [27]. No crystal structures of cyt bc_1 are available from human- or

plant pathogen sources, however the yeast enzyme has proved a useful and genetically amenable model in many instances [1,4,28-32].

The Q_o site within cyt *b* is composed from components encompassing the C-terminal domain of transmembrane helix C, surface helix cd1 and the region encompassing the "PEWY" (Pro_{271}-Glu-Trp-Tyr_{274}, yeast notation) loop/ef helix to transmembrane helix F1 (Fig. 3). It forms a large, bifurcated, and predominantly hydrophobic volume [33,34]. Cyt bc_1 has been co-crystallised with a variety of competitive inhibitors for the Qo site (see [10,34] and references therein, also [4]), but, despite extensive efforts, there are no atomic structures available for the enzyme with substrate ubiquinol bound at Q_o. Ligands binding within Q_o may be broadly classified as 'b_L distal' or 'b_L proximal' species depending on their positioning within the site with respect to haem b_L. b_L distal inhibitors, such as stigmatellin, n-nonyl quinoline N-oxide (NQNO), n-undecyl hydroxy dibenzothiazole (UHDBT) and atovaquone bind in a region of Q_o in close proximity to the ISP (Fig. 1), often forming a strong hydrogen bond to a histidine ligand (H181) of the [2Fe2S] cluster, and restricting the movement of the ISP-ED in crystallographic studies [10,19,34]. As such, this class of inhibitor may also be classified as 'Pf' ('P' referring to Q_p, an alternative nomenclature for Q_o (i.e. the *p*ositive side of the energy coupling membrane), with 'f' indicating that the ISP-ED is *f*ixed in position) [34]. These inhibitors may also alter the redox- and EPR spectroscopic properties of the [2Fe2S] cluster, a clue to their mode of action prior to the elucidation of the atomic structure of cyt bc_1. To complicate matters, it should be noted that not all b_L-distal/Pf inhibitors form H-bonding associations with the ISP-ED. Famoxadone (an oxazolidine-dione-containing synthetic fungicide) is a useful case-in-point here, demonstrating direct Q_o ligand/ISP-ED interactions are in themselves insufficient to retard the movement of the ISP-ED, and may arise from ligand-induced perturbation of the protein fold around this region of cyt *b* [35]. b_L-distal inhibitors may also form hydrogen-bonding interactions with the carboxylate moiety of E272 in the cyt *b* Q_o ef helix (this residue is in close proximity to haem b_L), causing this sidechain to rotate away from its inward pointing disposition in the uninhibited enzyme. This is observed with stigmatellin and NQNO, but not UHDBT [34,36].

In contrast to b_L-distal inhibitors, b_L-proximal inhibitors, such as the natural antibiotics myxothiazol and strobilurin, and synthetic fungicides such as azoxystrobin characteristically have hydrogen-bonding interactions with the backbone amide moiety of cyt *b* residue E272 at Q_o (Fig.

1), with the sidechain of this residue oriented away from the aqueous phase. Often such inhibitors possess a methoxyacrylate pharmacophore, or derivative of such [34,37]. Generally, b_L proximal inhibitors do not interact with the ISP-ED or affect its mobility, and so this class of compound are also referred to as 'Pm' (with 'm' indicating that the ISP-ED is mobile, or, at least, not docked at the IMS-facing surface of the Q_o site within cyt *b*) [34].

The Q_i site, located within cyt *b* on the opposite side of the IMM to Q_o, forms the site of quinone reduction within cyt bc_1. Structurally, it is formed from the C-terminal region of surface helix a, the N-terminal region of transmembrane helices A and E and the C-terminal regions of helices D (Fig. 3), and, in contrast to Q_o, contains no contributions from the ISP. Cyt bc_1 been cocrystallised with Q_i-bound substrate ubiquinone in the chicken, bovine and yeast enzyme, where it is observed that the benzoquinone moiety forms hydrogen bonds with Q_i residues H202 and S206 (yeast notation) [38-41]. Q_i-bound quinone is in close proximity (3.5Å shortest separation) to haem b_H, facilitating rapid electron transfer [12,17].

Cyt bc_1has been cocrystalised with a variety of Q_i inhibitors (QiI), such as the natural antibiotics antimycin A and ascochlorin, and synthetic pyridones [5,10,41-43]. These inhibitors tend to be structurally diverse molecules, and may not resemble simple variants of benzoquinones, as is often observed for Q_o inhibitors (QoI). Mechanistically, the redox chemistry catalysed at Q_i is less elaborate than that at Q_o [9,17], and there is no equivalent of the haem proximal/distal classification for QiI as observed with QoI. Notably, Q_i-inhibition can lead to increased superoxide production from cyt bc_1 due to electron accumulation on the low potential chain (and increased SQ_o occupancy) within this enzyme [44-46], which, due to the resulting oxidative stress, may increase the efficacy of such compounds as antimicrobial agents. It is often overlooked that b_L-proximal QoI (such as myxothiazol) can also stimulate ROS production by cyt bc_1, presumably as SQ_o generation can still proceed due to dual site occupancy at Q_o, allowing one-electron oxidation of substrate quinol by the ISP (but blocking reduction of cyt *b*) [47].

Finally, we note that some compounds, such as the fungal antibiotic ascochlorin, the synthetic fungicide ametoctradin and the synthetic antimalarial compound endochin ELQ-400 may act as *dual site* Q_o/Q_i inhibitors [31,32,43]. Such molecules are of particular interest as antimicrobial agents as cyt *b* mutation-based resistance is unlikely to develop without significant fitness cost to the target organism [48].

QoI/QiI binding may result in bathochromic shifts in the visible absorption spectra of reduced cytochrome b_L/b_H [37], and this technique is convenient test for the predictions of *in silico* modelling approaches. The b_L-proximal inhibitors strobilurin and myxoythiazol have been observed to induce 1-2 nm redshifts of haem b_L, shifting the absorption maximum of the α-band to 566 nm. A similar spectral shift is observed with the b_L-distal inhibitor stigmatellin (Fig. 1) [37]. At Q_i, the binding of the antagonist antimycin A induces a 2 nm bathochromic shift in the visible absorption spectrum of haem b_H, shifting the absorption maximum of the α-band to 564 nm. Relatedly, the phenomenon of 'oxidant-induced reduction' - the reduction of the low potential chain within cyt bc_1 in the presence of QiI and ascorbate or substrate quinol upon addition of an oxidant such as ferricyanide due to the bifurcated electron transfer chemistry at Q_o can also provide clues as to the mode of action of cyt bc_1 Q-site inhibitors [11,49,50]. We recommend the use of these relatively simple spectrophotometric measurements, which can be performed with crude membrane preparations, as complementary to *in silico* binding predictions. Study of the enzymology of inhibition in Q_o/Q_i site-directed mutants of yeast (and bacterial) cyt bc_1 can also provide useful information with regards to the mode of action of potential QoI/QiI [1,29,30,51].

Cytochrome bc_1 as a fungicide target in crop phytopathogens

Plant disease control is a major issue in agriculture. The fungicide market in Europe, for instance, represents € 1.8 bn/year; of this, € 1.3 bn/year are for wheat disease control [52]. A wide panel of fungicides are available with different modes of action and targets, such as the large group of fungal sterol biosynthesis inhibitors, the growing family of complex II inhibitors, or the cyt bc_1 inhibitors.

The QoI fungicides and the rapid spread of target site resistance

Cyt bc_1 is a successful target for agricultural fungicides, with most of the compounds in use being Q_o-site inhibitors (QoIs). They are (and have been) used to control a wide range of plant pathogen fungi belonging to the ascomycetes, basidiomycetes and oomycetes. Some of the pathogens are the causative agents of diseases of economically important crops, such as cereals and vines.

The QoIs available on the market include several synthetic strobilurins [53] such as azoxystrobin, dimoxystrobin, fluoxastrobin, kresoxim-methyl, picoxystrobin, pyraclostrobin, trifloxystrobin, but also the benzyl-carbamate pyribencarb, the oxazolidine-dione famoxadone and the imidazolone fenamidone. These compounds are likely to share the same binding mode as the resistance mutation G143A in the cyt *b* Q_o-site confers cross-resistance to all of these inhibitors.

The first QoI marketed for agricultural use, azoxystrobin, was launched in 1996. Unfortunately, its efficiency was rapidly challenged within a few years, with, resistant isolates reported in populations of pathogens, such as *Blumeria graminis*, (wheat and barley powdery mildew) [54] and *Plasmopara viticola*, (grape downy mildew) [55]. We will address additional fungal resistance mechanisms, namely the upregulation of alternative respiratory pathways and activity of membrane efflux pumps later in this review.

Fungal phytopathogen resistance to azoxystrobin was found to be caused by the cyt *b* mutation G143A in the Q_o site (Fig. 1, Fig. 3), and, interestingly, A143 is found natively in cyt *b* of the strobilurin-producing basidiomycete *Mycena galopoda* [56]. The G143A substitution has been now found in isolates from over 25 species of phytopathogenic fungi (see Fungicide Resistance Action Committee (FRAC): www.frac.info). As such, FRAC often recommend mixing two or more fungicides with differing modes of action to try and overcome this problem of resistance. The G143A mutation confers a high level of resistance that can result in a severe loss in disease control by QoIs. Inspection of the atomic structure of bovine cyt bc_1 with bound azoxystrobin indicates that replacement of G143 by alanine results in a destabilising steric clash with the MOA-bearing phenyl moiety of the fungicide. In yeast, G143A dramatically increases resistance to azoxystrobin (4,000x) but has no effect on cyt bc_1 enzymatic activity [29], indicating that the binding of substrate ubiquinol is not hindered by the mutation. The high level of resistance without penalty on the enzyme activity - combined perhaps with a heavy use of QoIs in fields and thus a strong selection pressure- could explain the rapid emergence and spread of G143A in many fungi.

In some species however, the exon-intron structure of the cyt *b* gene prevents the appearance of the G143A mutation [57]. In these species, an intron is located immediately after the codon for G143. When the G143-encoding codon GGT is located at the exon/intron boundary and is replaced by codon GCT (encoding alanine) the intron splicing is altered, resulting in a severe decrease in the amount of mature mRNA. Accordingly, the resulting loss of cyt *b* due to mutation at this

mRNA splice junction has been demonstrated in the yeast model [58]. G143A would thus have a deleterious effect in the intron-containing species, affect the fitness of the resistant cells and be counter-selected in field.

Three other cyt *b* mutations have been reported in isolates resistant to QoIs – including in the 'G143' intron-containing species. F129L, found for instance in *P.viticola* and *Pyrenophora teres* (Barley net blotch) [59] (and G137R, such as is found for in isolates of *Pyrenophora. Tritici-repentis* (wheat tan spot) and G137S, found in *Venturia effusa* (pecan scab) (Fig. 1, Fig. 3) [59,60].

G137 is at the N-terminal region of helix cd1, and is close to the interfacial region for ISP-ED binding. Substitution of glycine by arginine, a bulky and cationic residue is expected to lead to local distortion of the loop connecting helices C and cd1. In yeast, the mutation causes in a significant defect in respiratory growth and cytochrome bc_1 activity [61]. In pathogenic fungi, the non-conservative substitution may be expected to result in a fitness penalty, which could explain the rare occurrence of G137R/S in the field [59,60].

The side chain of F129 is oriented toward the hydrophobic cavity that facilitates substrate access to Q_o. The residue is involved in binding the hydrophobic tail of stigmatellin and also presumably that of ubiquinol [62]. In yeast, the F129L mutation has little effect on the enzyme activity but decreases its sensitivity to QoIs azoxystrobin and stigmatellin [29]. F129 participates in sidechain van der Waals associations with these inhibitors in the respective cytochrome bc_1 structures, and the F129L substitution removes stabilising aromatic-aromatic interactions between the protein and bound azoxystrobin. F129L is not as widely spread in plant pathogen fungi as G143A and confers a moderate level of resistance.

G143A, now widespread in fungi in the field, is thus a major problem as the mutation confers high level of resistance and cross-resistance to the whole family of QoIs in use, compromising their efficiency in disease control. As such, new compounds are needed that either target the Q_i site or bind at Q_o but in a different mode, circumventing G143A-mediated resistance.

Metyltetraprole is a novel QoI that is not affected by the resistance mutation G143A [63]. It is active against ascomycetes, for instance *Zymoseptoria tritici* (wheat leaf blotch), a major threat for wheat production in Western Europe. The compound has side chain similar to that of the synthetic strobilurin pyraclostrobin, but has a unique tetrazolinone-moiety. It is suggested that this

tetrazolinone-moiety will not form the same highly specific interactions with the Q_o-site as do other strobilurin-based QoIs and in consequence can accommodate changes in the target, such as G143A [64]. Thus, the steric clash due to G143A that can compromise the binding of QoIs would be limited by the unique size and shape of the tetrazolinone. The atomic structure of wt and G143A cytochrome bc_1 with bound metyltetraprole would be needed to confirm its distinct binding interactions with the target.

QiI fungicides in use and under development, and appearance of resistance mutations

To date, only three QiI fungicides have been commercialized and are oomycete-specific, namely the dimethyl-sulfonamides amisulbron and cyazofamid, and the triazolopyrimidine ametoctradin.

In the FRAC repertory of fungicides (www.frac.info), ametoctradin was listed as QoSI i.e. binding at the Q_o-site in a manner similar to stigmatellin but distinct to QoIs [6]. Further spectroscopic studies indicated that the compound could target both Q_o- and Q_i- sites [31] and the fungicide was re-classified as QioI (https://osf.io/qwg42/). However the appearance of the amectotradin resistance mutation S34L in the Q_i-site of *P.viticola* resistant isolates showed that the fungicide preferentially target the Q_i-site, which was confirmed by the study of the mutation in the yeast model [51,65]. Analysis of *in silico* docking of ametoctradin into a homology model of the Q_i-site of *P.viticola* suggest a binding mode similar to that of ubiquinol in yeast cyt bc_1. The aliphatic octyl- and ethyl substituents of ametoctradin are predicted to form stabilizing hydrophobic interactions with the sidechains of L17 (helix A), V194 and L198 (C-terminal region of helix D) (Fig. 3). The interactions between the amino-substituted triazolo-pyrimidinyl headgroup of the fungicide and the Q_i-site appear more hydrophilic, with a putative H-bond with the carboxylate sidechain of residue D229. A weaker H-bonding interaction between this amino moiety of ametoctradin and the serinyl sidechain of S34 is also predicted, which would be lost when serine is replaced by leucine. In addition, the bulky leucine is expected to sterically destabilize the fungicide binding, which would explain the resistance [31,51].

A cyazofamid resistance mutation was reported in field isolates of *P. viticola*. Interestingly, the mutation is short sequence duplication of six nucleotides resulting in the insertion of two residues E203-DE-V204 [66], located in the linker region between helices D and E, proximal to the

benzoquinone headgroup of Q_i-site bound quinone in yeast cyt bc_1. The insertion is likely to perturb the local fold around this region, and interfere with cyazofamid access or binding into the Q_i-site.

Fenpicoxamid is a new QiI active against a broad range of ascomycetes, such as the wheat pathogen *Z.tritici* . It is still under commercial development. Fenpicoxamid is derived from UK-2A, a natural product of *Streptomyces sp*. that is structurally related to antimycin [67]. In *Z.tritici*, fenpicoxamid is readily converted into UK-2A by removing the isopropylcarboxymethylether group [68]. UK-2A is 100-fold more potent than fenpicoxamid in inhibiting cyt bc_1 [69]. Using the yeast model, three cytochrome *b* mutations causing fenpicoxamid resistance were identified, L198F and G37C and N31K [69]. Notably, mutations of these residues L198, N31 and G37 have been reported to cause resistance to different Q_i-site inhibitors in different organisms. Residue G37, in particular, seems a hot-spot of resistance mutations [51].

The binding of UK-2A to yeast cyt bc_1 has been modelled *in silico* [69]. The results suggested a structural overlap between UK-2A and antimycin A in the Q_i binding pocket, with differences, in particular the pyridine head of UK-2A is flipped by 180 degrees. In this model, the N atom in the pyridine ring is protonated and can form a salt bridge with the carboxyl group of D229, a key residue in Q_i-site inhibitor binding. However, in contrast to UK-2A, other Q_i-site inhibitors form a hydrogen bond with an O atom of D229. It is likely that the local electrostatic environment around D229 is affected by the replacement of the nearby residue N31 by lysine (N31K), disrupting the salt bridge (or bound water molecules, which may also interact with the Q_i antagonist [69]) and in consequence weakening the inhibitor binding. Destabilising steric hindrance is likely to explain the resistance caused by G37C and L198F, as the substitutions result in bulkier residues.

Alternative QoI/QiI resistance mechanisms in fungal phytopathogens

In addition to mutations in the inhibitor binding site within cyt *b* that account for most of the cases of reported resistance, other mechanisms may induce resistance towards QoIs and QiIs, such as increased efflux of fungicides and activation of a mitochondrial alternative oxidase (AOX) [70 - 72]. These mechanisms need to be taken into account in the strategies for monitoring and controlling the development of resistance.

Increased drug efflux is less prevalent and result in lower resistance level than cyt *b* mutations. It is caused by the upregulation of membrane transporters. As these efflux pumps can often transport different compounds, their increased activity lead to multiple drug resistance (MDR). In *Z.tritici*, for instance, MDR was reported and found be caused by the overexpression of the transporter MFS1, induced by insertions in the promoter of its encoding gene [72,73].

AOX forms an alternative respiratory pathway within the mitochondria of the phytopathogen which may be upregulated when cyt bc_1 is inhibited. AOX is a single-subunit, (non-haem) di-iron containing monotopic membrane protein which functions as a non-protonmotive quinol oxidase, which is widespread in plant, fungal and protist mitochondria (but notably absent from the *Plasmodium* sp.) [74-76]. The activity of AOX allows ubiquinol-linked respiration from NADH (via mitochondrial complex I) to oxygen, bypassing the inhibition of cyt bc_1, although at much reduced energetic efficiency. 4 protons may be expected to be pumped into the IMS per 2 electrons transferred to oxygen in this alternative respiratory pathway due to the activity of protonmotive complex I alone (i.e. $4H^+/2e^-$) [75]. This represents a significant decrease from the $10H^+/2e^-$ yield expected for cyt bc_1/cytochrome *c* oxidase-linked respiration. Putatively AOX-linked fungicide resistance was first noted in laboratory-generated strains of *Z. tritici*, that were resistant to the (then) newly developed QoI azoxystrobin [77], and has subsequently has been observed in QoI/QiI-treated field isolates of the phytopathogens *P. viticola*, *Z. tritici, Magnaporthe grisea* and *Mycosphaerella fijensis* [65,78-80]. *In vitro* studies suggest that, in the absence of selective pressure, AOX overexpression in *P. viticola* sporangia comes with an associated fitness penalty [6], presumably due to the decreased energetic efficiency of mitochondrial respiration as outlined above. Accordingly, the fungal preinfection stages of spore germination and host penetration may be unlikely to develop AOX-associated QoI/QiI resistance due to the ATP demand of these processes [53,70,77,80]. *In vitro*, AOX activity can be inhibited by the benzhydroxyamic compound salicylhydroxamic acid (SHAM), a presumed competitive inhibitor for ubiquinol. SHAM is a relatively poor inhibitor of the AOX, with an inhibition constant (K_i) of 21 μM against the *Trypanosoma brucei* enzyme (as measured by glycerophosphate-linked oxygen uptake assay) [81]. As an anti-fungal agent, SHAM has also been observed to act synergistically with QoI inhibitors *in vitro*, but this response is species (and QoI) dependent [65,70,82]. Unfortunately, SHAM is a relatively non-specific inhibitor and poorly taken up by plants, and so is unsuitable for use in the field [70]. It must also be noted that the native AOX activity is important for maintaining

redox (and metabolite) homeostasis in plants, and inhibition of this enzyme may be deleterious under osmotic- and light stress conditions [83,84]. Nevertheless, the intriguing possibility exists of the development of dual fungal cyt bc_1/AOX inhibitors, as compounds such as the quinoline aurachins, produced by the myxobacterium *Stigmatella aurantiaca*, are inhibitors of both enzymes [85-88]. We note also the potential for complex I/cyt bc_1 inhibition for fungicidal activity as Δp would be expected to be severely diminished under such circumstances, regardless of the activity of AOX. Complex I-targeting fungicides are not in widespread use, although the methylpyrimidin-4-amine compound diflumetorim is approved for use in Japan for treatment of rust and powdery mildew infection of ornamental crops [89].

The QoI alkoxyimionacetamide fungicide SSF-126 has been reported to increase superoxide production in *M. grisea* [90], and although the Q_o site of cyt bc_1 is the likely source of origin (presumably SSF-126 is acting as a b_L-proximal inhibitor in this instance, or there is cross reactivity of this compound with Q_i), this has not been tested directly. AOX expression was observed to be strongly induced on treatment with SSF-126, although interestingly the addition of exogenous hydrogen peroxide was also observed to increase AOX mRNA transcript levels [78]. Earlier studies reported a possible ROS-associated link with AOX expression in the yeast *Hansenula anomala* (syn. *Pichia anomala*) [91], and more recently, in tomato leaves [92]. The signalling pathway controlling this mechanism is unknown, but it potentially may be exploited in the development of future cyt bc_1-targeted fungicides (by, for instance, stimulating mitochondrial catalase or peroxidase expression) to minimise AOX-associated resistance mechanisms.

The significance of phytopathogen AOX activity with regards to QoI/QiI fungicide resistance in the field has been debated [6,70]. Its increasing prevalence, however, warrants close attention, particularly as this respiratory shunt (and MDR activity, as described above) may facilitate the development of QoI/QiI-resistant cyt *b* mutants [65].

Finally, we note the potential of the new, bifunctional 'hybrid' antifungal agents under development, that combine strobilurin- and aromatic amide pharmacophores. Such compounds are thus capable of targeting both cyt bc_1 and succinate dehydrogenase (an additional antipathogenic target). These hybrid compounds have demonstrated notable efficacy against the plant pathogens *Pyricularia oryzae* and *Sclerotinia sclerotiorum* under laboratory conditions [93].

382

383 **Cyt bc_1 as a chemotherapeutic target of the human malaria parasite**

384 The cytochrome bc_1 complex of the human malaria parasite *Plasmodium falciparum* has a number
385 of unique features that enable drug selectivity in humans. Notably, a four-residue deletion in the
386 cd2 helix (Fig. 3) of plasmodial cyt *b*, a region of the protein in close proximity to key structural
387 components of the Q_o site and the mobile domain of the ISP may modify the conformation of Q_o
388 in the parasite, forming an exploitable element for antagonist selectivity. Sequence differences
389 between Plasmodia and humans in the C-terminal region of the E-ef loop of cyt *b* (notably the loss
390 of histidine and lysine residues in the parasite), a region of the protein adjacent to catalytically
391 essential ef helix element of Q_o, may also help drive drug selectivity [2,94,95].

392

393 Besides contributing to the mitochondrial Δp [76,96-98], the quinol oxidase function of cyt bc_1
394 performs an important role within *Plasmodium* mitochondria, oxidising the electron acceptor pool
395 for DHODH-mediated pyrimidine biosynthesis. As noted previously, the mitochondria of
396 *Plasmodium* sp. lack the AOX found in plants, fungi and other protists, and so are reliant upon cyt
397 bc_1 activity for this function [76]. During the intraerythrocytic stage of parasite development
398 within the human host, provision of quinol oxidase function is believed to be essential for parasite
399 survival. Consistent with this, inhibition of cyt bc_1 results in an increase in carbamoyl-aspartate
400 and a reduction in UTP, CTP, and dTTP [3,99 -101]. Further evidence of an essential link between
401 mitochondrial function and pyrimidine biosynthesis is supported by the generation of an
402 atovaquone-resistant phenotype in transgenic *P. falciparum* parasites expressing ubiquinone-
403 independent yeast DHODH [102]. Inhibition of *Plasmodium* cyt bc_1 has been shown to affect the
404 conversion of fumarate to aspartate, further linking mitochondrial function with pyrimidine
405 biosynthesis and also possibly purine metabolism [103] .

406

407 Inhibition of *P. falciparum* cyt bc_1 during the intraerythrocytic (blood) stages of parasite
408 development result in a relatively slow death phenotype compared with other antimalarials such
409 as artemisinin and semisynthetic derivatives thereof [3,104,105]. This feature appears to be
410 consistent with other mitochondrially-acting antimalarials and is possibly due to the drug acting
411 only on late trophozoites and not on the earlier 'ring' stages [3,106,107]. Inhibition of *P.*
412 *falciparum* cyt bc_1 has also been validated against liver stages of the malaria parasite, resulting in

the utility of any developed inhibitors as prophylactic agents; however, inhibition of the parasite cyt bc_1 is not believed to be active against 'dormant' *P. vivax*/*ovale* hypnozoites and therefore not suitable for potential radical cure of relapse malaria [108,109].

Development and pharmacology of the cyt bc_1 Q_o inhibitor atovaquone

Atovaquone (Fig. 4) is the prototypal inhibitor of the *Plasmodium* cyt bc_1 that was successfully developed and registered for clinical use [110]. Currently, atovaquone is used as a fixed-dose combination with proguanil (Malarone) for the treatment of children and adults with uncomplicated malaria or as a chemoprophylactic agent for preventing malaria in travellers [108 ,111]. In recent years in the USA, Malarone has been estimated to account for *ca*.70% of all antimalarial pre-travel prescriptions [112]. Atovaquone is the product of over 50 years of research-intensive efforts to develop a safe and effective antimalarial [110]. Much of what is known of the essentiality of the parasite cyt bc_1 target and the physiological role of cyt bc_1 in mitochondrial function and linked biosynthetic pathways e.g. pyrimidine pathway (see section 3.0), is through the use of atovaquone.

Atovaquone binding to cyt *b* was initially hypothesised based on studies performed on model organisms and molecular modelling. These studies, which include electron paramagnetic resonance spectroscopy of the Rieske [2Fe2S] cluster, site-directed mutagenesis of model organism cyt *b* and gene sequencing of atovaquone-resistant *Plasmodium* species, demonstrate that atovaquone is most likely a competitive inhibitor of the parasite's cyt *b* Q_o site [1,2]. These studies were further supported by the demonstration using the X-ray structure of mitochondrial cyt bc_1 from *S. cerevisiae*, of atovaquone bound in the b_L-distal region of the Q_o site, at 3.0-Å resolution [4]. This study again confirmed the critical role of a polarized H-bond to His181 of the extrinsic domain of the Rieske protein that interacts with the ionized hydroxyl group of the drug. The sidechain of PEWY-residue Y279 (Fig. 1, Fig. 3) provides an important (and orienting) aromatic-aromatic interaction with the hydroxynaphthoquinone moiety of the drug, stabilising its binding within Q_o. The carbonyl groups of the Q_o-bound atovaquone molecule do not appear to be directly involved in H-bonding associations with the polypeptide backbone of cyt *b*, with the glutamyl sidechain of E272 pointing away from the drug, and towards haem b_L, in a manner reminiscent of that for the interaction with HDBT [36].

Malarone drug failure has been associated with atovaquone resistance, specifically with a missense point mutation at position 279 in cyt *b* (yeast notation, corresponding to 268 in the *P. falciparum* protein sequence), exchanging tyrosine for serine or cysteine (Y279S/C) or, less frequently, asparagine (Y279N) [1,113-117]

Position 279 in cyt *b* is highly conserved across all phyla and is located within the 'ef' helix component of the Q_o site (Fig. 1, Fig. 3), which is putatively involved in ubiquinol binding. The resultant atovaquone-resistant growth IC_{50} (half-maximal inhibitory concentration) phenotype of these mutants is some 1000-fold higher than susceptible strains; however, this is accompanied by a ~40% reduction in the V_{max} of cyt bc_1, suggestive of a significant fitness cost to the parasite [48]. We note that the Y279S mutation in *P. falciparum* confers weak cross-resistance to Q_o b_L-proximal inhibitor myxothiazol *in vitro* [48] (although this naturally-occurring antibiotic is unsuitable for use as an antimalarial agent). Interestingly, the G143A resistance mutation, as discussed earlier, and so prevalent in fungal phytopathogens, has yet to be observed in laboratory or field isolates of this organism.

Atovaquone monotherapy gives rise to *de novo* resistance very rapidly [118,119]. The underlying reason for this phenomenon has not been determined but pharmacodynamic/pharmacokinetic considerations as well as the multiple copy number of mtDNA (*ca*. 30 in *P. falciparum* and up to 150 in *P. yoelli* [120]) and the effect of an increased mutation rate of mitochondrially encoded genes have been discussed as potential contributing factors[110]. Whilst *de novo* resistance to atovaquone can occur rapidly in the blood stages of *P. falciparum*, malaria transmission studies suggests that resistant parasites harbouring specific cyt *b* mutations are not able to complete their development in the mosquito and are therefore unlikely to spread in the field [121].

A further notable recent development has been in the formulation of atovaquone slow-release strategies for chemoprotection. In rodent malaria models, atovaquone solid drug nanoparticles have been demonstrated to confers long-lived prophylaxis against malaria [122]. Pharmacokinetic-pharmacodynamic analysis indicates that if translated to humans this could potentially result in protection for at least one month after a single administration.

Development of second-generation *P. falciparum* cyt bc_1 inhibitors: pyridones, acridinediones, acridones and quinolones

Whilst the development of atovaquone gave rise to a new antimalarial therapy, its sub-optimal efficacy when used for malaria treatment (versus prophylaxis), the cost and complexity of synthesis resulting in a high cost of goods, as well as the observed rapid emergence of parasite resistance, limited its potential use for the treatment of patients in malaria endemic settings [110]. However, the malaria parasite cyt bc_1 offered a rare opportunity to drug developers as one of the few known validated drug targets resulting in the development of several inhibitor chemotypes.

Pyridones have been shown to possess antimalarial activity since the 1960's with the demonstration that clopidol possessed antimalarial efficacy against chloroquine resistant parasites [2]. In the early 2000's, GSK Pharmaceuticals reported the pre-clinical development of pyridones targeting cyt bc_1 of *P. falciparum* displaying activity against atovaquone-resistant parasites [123]. Development of pyridones by GSK containing an atovaquone-like bicyclic side chain gave rise to a clinical candidate GSK932121 (Fig. 4) which entered Phase 1 clinical trials in 2008[124]. However the trial was suspended due to the concurrent discovery of cardiotoxicity in animal studies dosed with the phosphate ester of the drug [125]. The toxicity was attributed to higher systemic exposure of the parent drug which was later confirmed when similar toxicity was observed in rats dosed with the parent drug by the intraperitoneal route. A subsequent study in which bovine cyt bc_1 was co-crystallised with the GSK932121 and other 4(1H)-pyridone class of inhibitors, demonstrated that these inhibitors do not bind at the Q_o site but bind at the Q_i site, thereby providing an explanation for the apparent activity against atovaquone-resistant parasites (harbouring Q_o-site mutations) [5]. However, the study also demonstrated a much lower therapeutic index of the pyridones against bovine cyt bc_1 compared to atovaquone, thereby also providing a molecular explanation for the cardiotoxicity and eventual failure of GSK932121 in the phase-1 clinical trial.

Nevertheless, the Q_i site of *P. falciparum* cyt bc_1 offers itself as a promising target for drug development, particularly in combination with a Q_o-directed antagonist, such as atovaquone. We present a protein sequence alignment of the cyt *b* Q_i site from *P. falciparum* in comparison with

yeast and selected vertebrates in Fig. 5. This figure also highlights residues in the atomic structure of bovine cyt *b* (PDB accessions 1NTK, 4D6T and 4D6U in hydrogen-bonding or hydrophobic (sidechain/ligand) interaction with antimycin and the 4(1H)-pyridone-class inhibitors GW844520 and GSK932121 [5,35]. The N-terminal region of transmembrane helix E within *P. falciparum* cyt *b* Q_i appears to offer considerable sequence diversity compared to mammalian counterparts, which may form exploitable differences for drug development. In particular, we highlight the single residue deletion in the loop connecting helices D and E, and the presence of aliphatic- for ionic sidechain substitutions at L206, L217 and K220 (*P. falciparum* notation) for aspartate, lysine and leucine respectively in the human sequence data at the N-terminus of transmembrane helix E. Y211/N213 in the parasite sequence in the same region also appear to offer significant steric (and electrostatic) diversity from the His/Tyr dyad at the equivalent position in the human sequence. Given the considerable challenge of obtaining an atomic structure for *P. falciparum* cyt bc_1, it is likely that yeast cyt *b* side-directed mutants may provide suitable surrogates for the study of antagonist binding at Q_i.

Drugs based on the acridine chemotype have a long history in malaria chemotherapy, indeed mepacrine was the first synthetic antimalarial blood schizontocide used clinically [126] and the related drug pyronaridine is still in use today in the form of Pyramax (pyronaridine-artesunate combination). Additional acridine derivatives include the acridones and the dihydroacridinediones, all of which display potent antimalarial activity e.g. [127] Whilst the antimalarial efficacy of acridine congeners has been shown to derive from their ability to bind haem and thereby interfere with the parasite process of haem crystallisation [94,128-132],some potent dihydroacridinediones and acridones have been demonstrated to inhibit malaria parasite O_2-consumption [133]and specifically inhibit parasite cyt bc_1 [94,127] . Experiments performed with yeast manifesting mutations in cyt bc_1 reveal that binding of dihydroacridinediones is directed to the quinol oxidation site (Q_o) of cyt bc_1 [94].

Quinolones have been studied extensively as bc_1-targeting antimalarials [2,95,134]. A comprehensive set of alkyl- and alkoxy 4(1H)-quinolones have been synthesised in an effort to determine the structure activity relationship (SAR) for antimalarial efficacy against asexual *P. falciparum* parasites, including atovaquone-resistant lines [135]. This work led to the discovery of

ELQ-300 and P4Q-391 which were eventually selected as the preclinical candidate and backup molecule respectively, by the Medicines for Malaria Venture (MMV) [136]. ELQ300 and P4Q-391 (Fig. 4) were developed based on endochin, which was discovered over 70 years ago [137]. However whilst endochin and related alkyl-4(1H)quinolones possess antimalarial efficacy, the barrier to development was the metabolic instability due to the long alkyl chain. Replacement of the alkyl chain by the side chain from the previously described GSK pyridone series [124] proved to be a breakthrough for this chemotype as the molecules demonstrated improved metabolic stability while retaining antimalarial efficacy. Crucially ELQ300 displays improved selectivity over human cyt bc_1 relative to the withdrawn pyridone series [136]. Inhibition of the parasite cyt bc_1 is believed to be at the Q_i site (Fig. 5) [5], probably as a consequence of the QSAR being directed against atovaquone-resistant parasites harbouring Q_o-site mutations. Interestingly, *in vitro* isobole analysis of atovaquone and ELQ300 combination efficacy displays a synergistic interaction, suggesting that Q_o and Q_i inhibitors are a favourable combination strategy.

As outlined earlier, dual-site resistance may be expected to be unlikely to develop due to the increased probability of an associated organismal fitness penalty [48]. Additionally, inhibition at Q_i is likely to lead to increased (superoxide-linked) oxidative stress within the pathogenic organism [46]. (We also note that putative dual *P. falciparum* cyt bc_1/NADH dehydrogenase inhibitors, such as the quinolone lead compound SL-2-25 [3] may also increase oxidative stress within the pathogen due to dehydrogenase-associated flavosemiquinone formation [138]. In addition, the Q_o-Y279S mutation does not confer appreciable resistance to this compound, nor to the related compound CK-2-68 [3,139]).

The ELQ class however does have some limitations, most notably the class suffers from poor aqueous solubility which *in vivo* is reflected in limited absorption and bioavailability – whilst this is not an issue in terms of reaching adequate *in vivo* exposures for efficacy, it is not possible to establish maximum tolerated doses to establish a therapeutic index. This issue stalled ELQ-300 development. However more recently prodrug approaches are attempting to overcome this issue. ELQ-331, an alkoxycarbonate ester of ELQ-300, is currently the lead prodrug that is reported to have significantly increased ELQ-300 exposure after oral dosing [140]. ELQ-331 is currently

advancing pre-clinical development as an oral formulation and is also being progressed as a long-acting injectable chemoprotection agent [141].

Other notable quinolone-based cyt bc_1 inhibitors developments include the identification of decoquinate [142] and quinolone esters [143], these projects have thus far not developed further as they have not demonstrated superiority over existing molecules under development described above.

Cyt bc_1 as an antipathogenic target - general outlook and future prospects

The above discussion about atovaquone makes it clear that the development of parasite resistance is a concern for the continuing efficacy of cyt bc_1 Q_o-targeted antimalarial agents. However, this problem does not seem insurmountable, given the potential for the dual-site (Q_o/Q_i) combination therapy, or indeed, the development of true dual-site inhibitors, as proposed for the mode of action of the endochin compound ELQ-400 in yeast models of *P. falciparum* cyt bc_1 [32]. Furthermore, the lack of cross resistance to lead compounds such as quinolone Q_o-antagonist CK-2-68 in the atovaquone-resistant *P. falciparum* strain TM90C2B [3] offers hope for the future exploitation of the Q_o site as an antimalarial chemotherapeutic target

With regards to fungal phytopathogens the question of QoI/QiI efficacy is even more pressing, in light of the additional issues of the inducible AOX-mediated respiratory bypass and MDR efflux pumps. Nevertheless, and as with human malaria parasite, the development of novel fungicidal QoI/QiI continues, particularly with the example set by the new QiI for treatment of Ascomycete plant pathogens, fenpicoxamid [69], insensitive to G143A-mediated resistance. As above, dual-site (Q_o/Q_i) fungicidal activity would seem to offer the best chances against developing viable resistant strains, particularly if the issue of G143A resistance can be bypassed by the development of non-strobilurin based inhibitors, occupying the b_L-distal region of Q_o. The recent exciting development of 'hybrid' bi-functional fungicides also deserves close observation [93]. Finally, we note that in the absence of suitable AOX inhibitors, the spread of respiratory bypass-based inhibition must be carefully monitored, and the necessity of the energetic role played by AOX during the various developmental stages of fungal growth.

Acknowledgments

N.F. acknowledges support from grant DE-SC0007101 from the Photosynthetic Systems program from the Division of Chemical Sciences, Geosciences, and Biosciences, Office of Basic Energy Sciences of the U.S. Department of Energy.

References

[1] Kessl JJ, Meshnick SR and Trumpower BL (2007). Modeling the molecular basis of atovaquone resistance in parasites and pathogenic fungi. *Trends Parasitol* **23**, 494-501.

[2] Barton V, Fisher N, Biagini GA, Ward SA and O'Neill PM (2010). Inhibiting *Plasmodium* cytochrome bc_1: A complex issue. *Curr Opin Chem Biol* **14**, 440-446.

[3] Biagini GA *et al.* (2012). Generation of quinolone antimalarials targeting the *Plasmodium falciparum* mitochondrial respiratory chain for the treatment and prophylaxis of malaria. *Proc Natl Acad Sci U S A* **109**, 8298-303.

[4] Birth D, Kao WC and Hunte C (2014). Structural analysis of atovaquone-inhibited cytochrome bc_1 complex reveals the molecular basis of antimalarial drug action. *Nature Commun* **5**, 4029.

[5] Capper MJ *et al*. (2015) Antimalarial 4(1H)-pyridones bind to the Q_i site of cytochrome bc_1. *Proc Natl Acad Sci U S A* **112**, 755-760.

[6] Fehr M, Wolf A and Stammler G (2015). Binding of the respiratory chain inhibitor ametoctradin to the mitochondrial bc_1 complex. *Pest Manag Sci* **72**, 591-602.

[7] Zhou Y *et al.* (2015). Resistance mechanisms and molecular docking studies of four novel QoI fungicides in *Peronophythora litchii*. *Sci Rep* **5**, 17466.

[8] Berry EA, Guergova-Kuras M, Huang LS and Crofts AR (2000). Structure and function of cytochrome *bc* complexes. *Annu Rev Biochem* **69**, 1005-75.

[9] Crofts AR (2004). The cytochrome bc_1 complex: Function in the context of structure. *Annu Rev Physiol* **66**, 689-733.

[10] Xia D, Esser L, Tang W-K, Zhou F, Zhou Y, Yu L and Yu C-A (2013). Structural analysis of cytochrome bc_1 complexes: Implications to the mechanism of function. *Biochim Biophys Acta* **1827**, 1278-1294.

627 [11] Trumpower BL (1990). The protonmotive Q cycle. Energy transduction by coupling of
628 proton translocation to electron transfer by the cytochrome bc_1 complex. *J Biol Chem* **265**,
629 11409-12.
630 [12] Zhang H, Chobot SE, Osyczka A, Wraight CA, Dutton PL and Moser CC (2008). Quinone
631 and non-quinone redox couples in Complex III. *J Bioenerg Biomembr* **40**, 493-499.
632 [13] Mitchell P (1975). Protonmotive Q-cycle - general formulation. *FEBS letters* **59**, 137-139.
633 [14] Crofts AR, Shinkarev VP, Kolling DRJ and Hong S (2003). The modified Q-cycle explains
634 the apparent mismatch between the kinetics of reduction of cytochromes c_1 and b_H in the
635 bc_1 complex. *J Biol Chem* **278**, 36191-201.
636 [15] Osyczka A, Moser CC and Dutton PL (2005). Fixing the Q cycle. *Trends Biochem Sci* **30**,
637 176-82.
638 [16] Cape JL, Bowman MK and Kramer DM (2006). Understanding the cytochrome *bc*
639 complexes by what they don't do. The Q-cycle at 30. *Trends Plant Sci* **11**, 46-55.
640 [17] Crofts AR *et al.* (2008). The Q-cycle reviewed: How well does a monomeric mechanism
641 of the bc_1 complex account for the function of a dimeric complex? *Biochim Biophys Acta*
642 **1777**, 1001-19.
643 [18] Swierczek M, Cieluch E, Sarewicz M, Borek A, Moser CC, Dutton PL and Osyczka A
644 (2010). An electronic bus bar lies in the core of cytochrome bc_1. *Science* **329**, 451-4.
645 [19] Crofts AR, Guergova-Kuras M, Huang L, Kuras R, Zhang Z and Berry EA (1999).
646 Mechanism of ubiquinol oxidation by the bc_1 complex: Role of the iron sulfur protein and
647 its mobility. *Biochemistry* **38**, 15791-806.
648 [20] Darrouzet E and Daldal F (2002). Movement of the iron-sulfur subunit beyond the *ef* loop
649 of cytochrome *b* is required for multiple turnovers of the bc_1 complex but not for single
650 turnover Q_o site catalysis. *J Biol Chem* **277**, 3471-6.
651 [21] Darrouzet E and Daldal F (2003). Protein-protein interactions between cytochrome *b* and
652 the Fe-S protein subunits during QH_2 oxidation and large-scale domain movement in the
653 bc_1 complex. *Biochemistry* **42**, 1499-507.
654 [22] Crofts AR, Hong S, Wilson C, Burton R, Victoria D, Harrison C and Schulten K (2013).
655 The mechanism of ubihydroquinone oxidation at the Q_o-site of the cytochrome bc_1
656 complex. *Biochim Biophys Acta* **1827**, 1362-1377.

[23] Crofts AR, Lhee S, Crofts SB, Cheng J and Rose S (2006). Proton pumping in the bc_1 complex: A new gating mechanism that prevents short circuits. *Biochim Biophys Acta* **1757**, 1019-1034.

[24] Rutherford AW, Osyczka A and Rappaport F (2012). Back-reactions, short-circuits, leaks and other energy wasteful reactions in biological electron transfer: Redox tuning to survive life in O_2. *FEBS Lett* **586**, 603-616.

[25] Pietras R, Sarewicz M and Osyczka A. (2016) Distinct properties of semiquinone species detected at the ubiquinol oxidation Q_o site of cytochrome bc_1 and their mechanistic implications. *J Roy Soc Interface* **13**, 20160133.

[26] Fisher N, Bowman M and Kramer DM (2016) Electron transfer reactions at the Q_o site of the cytochrome bc_1 complex: the good, the bad, and the ugly. In Cytochrome Complexes Evolution Structures, Energy Transduction, Signaling (Cramer WA and Kallas T, eds), pp. 419–434. Springer, Netherlands.

[27] Amporndanai K *et al.* (2018). X-ray and cryo-em structures of inhibitor-bound cytochrome bc_1 complexes for structure-based drug discovery. *IUCrJ* **5**, 200-210.

[28] Fisher N, Brown AC, Sexton G, Cook A, Windass J and Meunier B (2004). Modeling the Q_o site of crop pathogens in *Saccharomyces cerevisiae* cytochrome *b*. *Eur J Biochem* **271**, 2264-2271.

[29] Fisher N and Meunier B (2005). Re-examination of inhibitor resistance conferred by qo-site mutations in cytochrome *b* using yeast as a model system. *Pest Manag Sci* **61**, 973-8.

[30] Vallières C *et al.* (2012). HDQ, a potent inhibitor of *Plasmodium falciparum* proliferation, binds to the quinone reduction site of the cytochrome bc_1 complex. *Antimicrob Agent Chemother* **56**, 3739-3747.

[31] Dreinert A, Wolf A, Mentzel T, Meunier B and Fehr M (2018). The cytochrome bc_1 complex inhibitor ametoctradin has an unusual binding mode. *Biochim Biophys Acta* **1859**, 567-576.

[32] Song Z, Iorga BI, Mounkoro P, Fisher N and Meunier B (2018). The antimalarial compound ELQ-400 is an unusual inhibitor of the bc_1 complex, targeting both Q_o and Q_i sites. *FEBS Lett* **62**, 327-11.

[33] Crofts AR, Barquera B, Gennis RB, Kuras R, Guergova-Kuras M and Berry EA (1999). Mechanism of ubiquinol oxidation by the bc_1 complex: Different domains of the quinol

688 binding pocket and their role in the mechanism and binding of inhibitors. *Biochemistry* **38**,
689 15807-15826.
690 [34] Esser L, Quinn B, Li Y-F, Zhang M, Elberry M, Yu L, Yu C-A and Xia D (2004).
691 Crystallographic studies of quinol oxidation site inhibitors: A modified classification of
692 inhibitors for the cytochrome bc_1 complex. *J Mol Biol* **341**, 281-302.
693 [35] Gao X *et al.* (2002). The crystal structure of mitochondrial cytochrome bc_1 in complex
694 with famoxadone: The role of aromatic-aromatic interaction in inhibition. *Biochemistry* **41**,
695 11692-702.
696 [36] Palsdottir H, Lojero CG, Trumpower BL and Hunte C (2003). Structure of the yeast
697 cytochrome bc_1 complex with a hydroxyquinone anion Q_o site inhibitor bound. *J Biol Chem*
698 **278**, 31303-11.
699 [37] von Jagow G and Link TA (1986). Use of specific inhibitors on the mitochondrial bc_1
700 complex. *Meth Enzymol* **126**, 253-71.
701 [38] Berry EA, Huang LS, Zhang Z and Kim SH (1999). Structure of the avian mitochondrial
702 cytochrome bc_1 complex. *J Bioenerg Biomembr* **31**, 177-190.
703 [39] Hunte C, Koepke J, Lange C, Rossmanith T and Michel H (2000). Structure at 2.3Å
704 resolution of the cytochrome bc_1 complex from the yeast *Saccharomyces cerevisiae* co-
705 crystallized with an antibody Fv fragment. *Structure* **8**, 669-684.
706 [40] Gao X, Wen X, Esser L, Quinn B, Yu L, Yu C-A and Xia D (2003). Structural basis for
707 the quinone reduction in the bc_1 complex: A comparative analysis of crystal structures of
708 mitochondrial cytochrome bc_1 with bound substrate and inhibitors at the Q_i site.
709 *Biochemistry* **42**, 9067-80.
710 [41] Huang L-s, Cobessi D, Tung EY and Berry EA (2005). Binding of the respiratory chain
711 inhibitor antimycin to the mitochondrial bc_1 complex: A new crystal structure reveals an
712 altered intramolecular hydrogen-bonding pattern. **351**, 573-597.
713 [42] Zhang Z *et al.* (1998). Electron transfer by domain movement in cytochrome bc_1. *Nature*
714 **392**, 677-84.
715 [43] Berry EA, Huang L-s, Lee D-W, Daldal F, Nagai K and Minagawa N (2010). Ascochlorin
716 is a novel, specific inhibitor of the mitochondrial cytochrome bc_1 complex. *Biochim*
717 *Biophys Acta* **1797**, 360-370.

[44] Boveris A, Cadenas E and Stoppani AO (1976). Role of ubiquinone in the mitochondrial generation of hydrogen peroxide. *Biochem J* **156**, 435-444.

[45] Sun J and Trumpower BL (2003). Superoxide anion generation by the cytochrome bc_1 complex. *Arch Biochem Biophys* **419**, 198-206.

[46] Dröse S and Brandt U (2008). The mechanism of mitochondrial superoxide production by the cytochrome bc_1 complex. *J Biol Chem* **283**, 21649-21654.

[47] Muller FL, Roberts AG, Bowman MK and Kramer DM (2003). Architecture of the Q_o site of the cytochrome bc_1 complex probed by superoxide production. *Biochemistry* **42**, 6493-6499.

[48] Fisher N *et al.* (2012). Cytochrome *b* mutation Y268S conferring atovaquone resistance phenotype in malaria parasite results in reduced parasite bc_1 catalytic turnover and protein expression. *J Biol Chem* **287**, 9731-41.

[49] von Jagow G, Ljungdahl PO, Graf P, Ohnishi T and Trumpower BL (1984). An inhibitor of mitochondrial respiration which binds to cytochrome *b* and displaces quinone from the iron-sulfur protein of the cytochrome bc1 complex. *J Biol Chem* **259**, 6318-26.

[50] Brandt U, Schägger H and von Jagow G (1988). Characterisation of binding of the methoxyacrylate inhibitors to mitochondrial cytochrome *c* reductase. *Eur J Biochem* **173**, 499-506.

[51] Mounkoro P, Michel T, Benhachemi R, Surpateanu G, Iorga BI, Fisher N and Meunier B (2018). Mitochondrial complex III Q_i-site inhibitor resistance mutations found in laboratory selected mutants and field isolates. *Pest Manag Sci* **75**, 2107-2114.

[52] Torriani SFF, Melichar JPE, Mills C, Pain N, Sierotzki H and Courbot M (2015). *Zymoseptoria tritici*: A major threat to wheat production, integrated approaches to control. *Fungal Genet Biol* **79**, 8-12.

[53] Bartlett DW, Clough JM, Godwin JR, Hall AA, Hamer M and Parr-Dobrzanski B (2002). The strobilurin fungicides. *Pest Manag Sci* **58**, 649-662.

[54] Sierotzki H, Wullschleger J and Gisi U (2000). Point mutation in cytochrome *b* gene conferring resistance to strobilurin fungicides in *Erysiphe graminis* f. Sp. *Tritici* field isolates. *Pestic Biochem Physiol* **68**, 107-112.

[55] Heaney S, Hall A, Davis S and Olaya, G (2000) Resistance to fungicides in the QoI-STAR cross resistance group: current perspectives. In Brighton Crop Protection Conference-Pests and Diseases (Brighton, UK), pp. 755-762.

[56] Kraiczy P, Haase U, Gencic S, Flindt S, Anke T, Brandt U and von Jagow G (1996). The molecular basis for the natural resistance of the cytochrome bc_1 complex from strobilurin-producing Basidiomycetes to center Q_p inhibitors. *Eur J Biochem* **235**, 54-63.

[57] Grasso V, Palermo S, Sierotzki H, Garibaldi A and Gisi U (2006). Cytochrome *b* gene structure and consequences for resistance to Q_o inhibitor fungicides in plant pathogens. *Pest Manag Sci* **62**, 465-472.

[58] Vallières C, Trouillard M, Dujardin G and Meunier B (2011). Deleterious effect of the Q_o inhibitor compound resistance-conferring mutation G143A in the intron-containing cytochrome *b* gene and mechanisms for bypassing it. *Appl Environ Microbiol* **77**, 2088-2093.

[59] Sierotzki H, Frey R, Wullschleger J, Palermo S, Karlin S, Godwin J and Gisi U (2007). Cytochrome *b* gene sequence and structure of *Pyrenophora teres* and *P. tritici-repentis* and implications for QoI resistance. *Pest Manag Sci* **63**, 225-233.

[60] Standish JR, Brenneman TB and Stevenson KL (2019). Quantifying the effects of a G137S substitution in the cytochrome bc_1 of venturia effusa on azoxystrobin sensitivity using a detached leaf assay. *Plant Dis* **103**, 841-845.

[61] Song Z, Lalève A, Vallières C, McGeehan JE, Lloyd RE and Meunier B (2016). Human mitochondrial cytochrome *b* variants studied in yeast: Not all are silent polymorphisms. *Hum Mutat* **37**, 933-941.

[62] Wenz T, Covian R, Hellwig P, MacMillan F, Meunier B, Trumpower BL and Hunte C (2007). Mutational analysis of cytochrome *b* at the ubiquinol oxidation site of yeast complex III. *J Biol Chem* **282**, 3977-3988.

[63] Suemoto H, Matsuzaki Y and Iwahashi F (2019). Metyltetraprole, a novel putative complex III inhibitor, targets known QoI-resistant strains of *Zymoseptoria tritici* and *Pyrenophora teres*. *Pest Manag Sci* **75**, 1181-1189.

[64] Arakawa A, Kasai Y, Yamazaki K and Iwahashi F (2018). Features of interactions responsible for antifungal activity against resistant type cytochrome bc_1: A data-driven analysis based on the binding free energy at the atomic level. *PLoS ONE* **13**, e0207673-16.

[65] Fontaine S, Remuson F, Caddoux L and Barrès B (2019). Investigation of the sensitivity of plasmopara viticolato amisulbrom and ametoctradin in French vineyards using bioassays and molecular tools. *Pest Manag Sci* **50**, 3-9.

[66] Cherrad, S., Hernandes, C., Steva, H. and Vacher, S. (2018) Resistance de *Plasmopara viticola* aux inhibiteurs du complexe III : un point sur la caracterisation phenotypique et genotypique des souches. In 12th International Conference on Plant Diseases, (Tours, France), pp 449-459.

[67] Usuki Y, Tani K, Fujita K and Taniguchi M (2001). Uk-2A, B, C and D, novel antifungal antibiotics from *Streptomyces* sp. 517-02. VI(1). Structure-activity relationships of UK-2A. *J Antibiot* **54**, 600-602.

[68] Owen WJ *et al.* (2017). Biological characterization of fenpicoxamid, a new fungicide with utility in cereals and other crops. *Pest Manag Sci* **73**, 2005-2016.

[69] Young DH, Wang NX, Meyer ST and Avila-Adame C (2017). Characterization of the mechanism of action of the fungicide fenpicoxamid and its metabolite UK-2A. *Pest Manag Sci* **74**, 489-498.

[70] Wood PM and Hollomon DW (2003). A critical evaluation of the role of alternative oxidase in the performance of strobilurin and related fungicides acting at the Q_o site of complex III. *Pest Manag Sci* **59**, 499-511.

[71] Lucas JA, Hawkins NJ and Fraaije BA (2015). The evolution of fungicide resistance. Elsevier Ltd *Adv Appl Microbiol* **90**, 29-92/

[72] Omrane S, Audéon C, Ignace A, Duplaix C, Aouini L, Kema G, Walker A-S and Fillinger S (2017). Plasticity of the MFS1 promoter leads to multidrug resistance in the wheat pathogen *Zymoseptoria tritici*. *mSphere* **2**, 3-19.

[73] Omrane S, Sghyer H, Audéon C, Lanen C, Duplaix C, Walker A-S and Fillinger S (2015). Fungicide efflux and the mgmfs1 transporter contribute to the multidrug resistance phenotype in *Zymoseptoria tritici* field isolates. *Environ Microbiol* **17**, 2805-2823.

[74] Moore AL, Shiba T, Young L, Harada S, Kita K and Ito K (2013). Unraveling the heater: New insights into the structure of the alternative oxidase. *Annu Rev Plant Biol* **64**, 637-663.

[75] Young L, May B, Shiba T, Harada S, Inaoka DK, Kita K and Moore AL. (2016) Structure and mechanism of action of the alternative quinol oxidases. In Cytochrome Complexes

Evolution Structures, Energy Transduction, Signaling (Cramer WA and Kallas T, eds), pp. 375-394. Springer, Netherlands.

[76] Hayward JA and van Dooren GG (2019). Same same, but different: Uncovering unique features of the mitochondrial respiratory chain of apicomplexans. *Mol Biochem Parasit* **232**, 111204-8.

[77] Ziogas BN, Baldwin BC and Young JE (1997). Alternative respiration: A biochemical mechanism of resistance to azoxystrobin (ICIA 5504) in *Septoria tritici*. *Pestic Sci* **50**, 28-34.

[78] Yukioka H, Inagaki S, Tanaka R, Katoh K, Miki N, Mizutani A and Masuko M (1998). Transcriptional activation of the alternative oxidase gene of the fungus *Magnaporthe grisea* by a respiratory-inhibiting fungicide and hydrogen peroxide. *Biochim Biophs Acta* **1442**, 161-169.

[79] Sierotzki H, Parisi S, Steinfeld U, Tenzer I, Poirey S and Gisi U (2000). Mode of resistance to respiration inhibitors at the cytochrome bc_1 enzyme complex of *Mycosphaerella fijiensis* field isolates. *Pest Manag Sci* **56**, 833-841.

[80] Miguez M, Reeve C, Wood PM and Hollomon DW (2003). Alternative oxidase reduces the sensitivity of *Mycosphaerella graminicola* to QoI fungicides. *Pest Manag Sci* **60**, 3-7.

[81] Clarkson Jr AB, Grady RW, Grossman SA, McCallum RJ and Brohn FH (1981). *Trypanosoma brucei brucei*: A systematic screening for alternatives to the salicylhydroxamic acid-glycerol combination. *Mol Biochem Parasitol* **3**, 271-291.

[82] Liang H-J, Di Y-L, Li J-L, You H and Zhu F-X (2015). Baseline sensitivity of pyraclostrobin and toxicity of SHAM to *Sclerotinia sclerotiorum*. *Plant Dis* **99**, 267-273.

[83] Giraud E *et al.* (2008). The absence of alternative oxidase 1A in Arabidopsis results in acute sensitivity to combined light and drought stress. *Plant Physiol* **147**, 595-610.

[84] Del-Saz NF, Ribas-Carbo M, Mcdonald AE, Lambers H, Fernie AR and Florez-Sarasa I (2018). An *in vivo* perspective of the role(s) of the alternative oxidase pathway. *Trends Plant Sci* **23**, 206-219.

[85] Kunze B, Höfle G and Reichenbach H (1987). The aurachins, new quinoline antibiotics from myxobacteria: Production, physico-chemical and biological properties. *J Antibiot* **40**, 258-265.

[86] Uhrig JF, Jakobs CU, Majewski C, Acta ATBeB and 1994 (1994). Molecular characterization of two spontaneous antimycin a resistant mutants of *Rhodospirillum rubrum*. *Mol Biochem Parasitol* **1187**, 347-353.

[87] Hoefnagel MH, Wiskich JT, Madgwick SA, Patterson Z, Oettmeier W and Rich PR (1995). New inhibitors of the ubiquinol oxidase of higher plant mitochondria. *Eur Journal Biochem* **233**, 531-537.

[88] Ebiloma GU, Balogun EO, Cueto-Díaz EJ, de Koning HP and Dardonville C (2019). Alternative oxidase inhibitors: Mitochondrion-targeting as a strategy for new drugs against pathogenic parasites and fungi. *Med Res Rev* **39**, 1553-1602.

[89] Fujii K and Takakura S (1998). Pyricut (difulmetorim, UBF-002EC): A new fungicide for ornamental use. *Agrochem Japan* **72**, 14-16.

[90] Mizutani A, Miki N, Yukioka H, Tamura H and Masuko M P (1996) A possible mechanism of control of rice blast disease by a novel alkoxyiminoacetamide fungicide, SSF126. *Phytopathology* **86**, 295–300.

[91] Minagawa N, Koga S, Nakano M, Sakajo S and Yoshimoto A (1992). Possible involvement of superoxide anion in the induction of cyanide-resistant respiration in *Hansenula anomala*. *FEBS Lett* **302**, 217-219.

[92] Eprintsev AT, Mal'tseva EV, Shatskikh AS and Popov VN (2011). Involvement of hydrogen peroxide in the regulation of coexpression of alternative oxidase and rotenone-insensitive NADH dehydrogenase in tomato leaves and calluses. *Biol Bull* **38**, 36-41.

[93] Zuccolo M *et al.* (2019). Dual-active antifungal agents containing strobilurin and SDHI-based pharmacophores. *Sci Rep* **9**, 11377-12.

[94] Biagini GA *et al.* (2008). Acridinediones: selective and potent inhibitors of the malaria parasite mitochondrial bc_1 complex. *Mol Pharmacol* **73**, 1347-1355.

[95] Nixon GL, Pidathala C, Shone AE, Antoine T, Fisher N, O'Neill PM, Ward SA and Biagini GA (2013). Targeting the mitochondrial electron transport chain of *Plasmodium falciparum*: New strategies towards the development of improved antimalarials for the elimination era. *Future Med Chem* **5**, 1573-91.

[96] Srivastava IK, Rottenberg H and Vaidya AB (1997). Atovaquone, a broad spectrum antiparasitic drug, collapses mitochondrial membrane potential in a malarial parasite. *J Biol Chem* **272**, 3961-6.

[97] Biagini GA, Viriyavejakul P, O'Neill P M, Bray PG and Ward SA (2006). Functional characterization and target validation of alternative complex I of *Plasmodium falciparum* mitochondria. *Antimicrob Agent Chemother* **50**, 1841-51.

[98] Antoine T, Fisher N, Amewu R, O'Neill PM, Ward SA and Biagini GA (2014). Rapid kill of malaria parasites by artemisinin and semi-synthetic endoperoxides involves ros-dependent depolarization of the membrane potential. *J Antimicrob Chemother* **69**, 1005-16.

[99] Hammond DJ, Burchell JR and Pudney M (1985). Inhibition of pyrimidine biosynthesis *de novo* in *Plasmodium falciparum* by 2-(4-t-butylcyclohexyl)-3-hydroxy-1,4-naphthoquinone *in vitro*. *Mol Biochem Parasitol* **14**, 97-109.

[100] Seymour KK, Yeo AE, Rieckmann KH and Christopherson RI (1997). DCTP levels are maintained in *Plasmodium falciparum* subjected to pyrimidine deficiency or excess. *Ann Trop Med Parasitol* **91**, 603-9.

[101] Allman EL, Painter HJ, Samra J, Carrasquilla M and Llinas M (2016). Metabolomic profiling of the malaria box reveals antimalarial target pathways. *Antimicrob Agents Chemother* **60**, 6635-6649.

[102] Painter HJ, Morrisey JM, Mather MW and Vaidya AB (2007). Specific role of mitochondrial electron transport in blood-stage plasmodium falciparum. *Nature* **446**, 88-91.

[103] Bulusu V, Jayaraman V and Balaram H (2011). Metabolic fate of fumarate, a side product of the purine salvage pathway in the intraerythrocytic stages of *Plasmodium falciparum*. *J Biol Chem* **286**, 9236-45.

[104] White NJ (1997). Assessment of the pharmacodynamic properties of antimalarial drugs *in vivo*. *Antimicrob Agent Chemother* **41**, 1413-22.

[105] McCarthy JS *et al.* (2011). A pilot randomised trial of induced blood-stage *Plasmodium falciparum* infections in healthy volunteers for testing efficacy of new antimalarial drugs. *PLoS One* **6**, e21914.

[106] Collins KA et al. (2019). DSM265 at 400 milligrams clears asexual stage parasites but not mature gametocytes from the blood of healthy subjects experimentally infected with Plasmodium falciparum. Antimicrob Agents Chemother **63**, e01837-18

[107] McCarthy JS *et al.* (2017). Safety, tolerability, pharmacokinetics, and activity of the novel long-acting antimalarial DSM265: A two-part first-in-human phase 1A/1B randomised study. *Lancet Infect Dis* **17**, 626-635.

[108] Lalloo DG and Hill DR (2008). Preventing malaria in travellers. *BMJ* **336**, 1362-6.

[109] Dembele L *et al.* (2011). Towards an *in vitro* model of *Plasmodium* hypnozoites suitable for drug discovery. *PloS One* **6**, e18162.

[110] Nixon GL, Moss DM, Shone AE, Lalloo DG, Fisher N, O'Neill PM, Ward SA and Biagini GA (2013). Antimalarial pharmacology and therapeutics of atovaquone. J Antimicrob Chemother 68, 977-985.

[111] Osei-Akoto A, Orton LC and Owusu-Ofori S (2009). Atovaquone-proguanil for treating uncomplicated malaria. *Cochrane Database Syst Rev* **2005**, CD004529

[112] LaRocque RC *et al.* (2012). Global travepinet: A national consortium of clinics providing care to international travelers--analysis of demographic characteristics, travel destinations, and pretravel healthcare of high-risk us international travelers, 2009-2011. *Clin Infect Dis* **54**, 455-62.

[113] Korsinczky M, Chen N, Kotecka B, Saul A, Rieckmann K and Cheng Q (2000). Mutations in *Plasmodium falciparum* cytochrome *b* that are associated with atovaquone resistance are located at a putative drug-binding site. *Antimicrob Agents Chemother* **44**, 2100-8.

[114] Fivelman QL, Butcher GA, Adagu IS, Warhurst DC and Pasvol G (2002). Malarone treatment failure and in vitro confirmation of resistance of *Plasmodium falciparum* isolate from lagos, nigeria. *Malar J* **1**, 1.

[115] Schwartz E, Bujanover S and Kain KC (2003). Genetic confirmation of atovaquone-proguanil-resistant *Plasmodium falciparum* malaria acquired by a nonimmune traveler to East Africa. *Clin Infect Dis* **37**, 450-1.

[116] Musset L, Bouchaud O, Matheron S, Massias L and Le Bras J (2006). Clinical atovaquone-proguanil resistance of *Plasmodium falciparum* associated with cytochrome *b* codon 268 mutations. *Microbes Infect* **8**, 2599-604.

[117] Berry A, Senescau A, Lelievre J, Benoit-Vical F, Fabre R, Marchou B and Magnaval JF (2006). Prevalence of *Plasmodium falciparum* cytochrome *b* gene mutations in isolates imported from Africa, and implications for atovaquone resistance. *Trans R Soc Trop Med Hyg* **100**, 986-8.

931 [118] Chiodini PL, Conlon CP, Hutchinson DB, Farquhar JA, Hall AP, Peto TE, Birley H and
932 Warrell DA (1995). Evaluation of atovaquone in the treatment of patients with
933 uncomplicated *Plasmodium falciparum* malaria. *J Antimicrob Chemother* **36**, 1073-8.
934 [119] Looareesuwan S, Viravan C, Webster HK, Kyle DE, Hutchinson DB and Canfield CJ
935 (1996). Clinical studies of atovaquone, alone or in combination with other antimalarial
936 drugs, for treatment of acute uncomplicated malaria in thailand. *Am J Trop Med Hyg* **54**,
937 62-6.
938 [120] Vaidya AB and Arasu P (1987). Tandemly arranged gene clusters of malarial parasites that
939 are highly conserved and transcribed. *Mol Biochem Parasitol* **22**, 249-57.
940 [121] Goodman CD *et al.* (2016). Parasites resistant to the antimalarial atovaquone fail to
941 transmit by mosquitoes. *Science* **352**, 349-53.
942 [122] Bakshi RP *et al.* (2018). Long-acting injectable atovaquone nanomedicines for malaria
943 prophylaxis. *Nat Commun* **9**, 315.
944 [123] Xiang H *et al.* (2006). Preclinical drug metabolism and pharmacokinetic evaluation of
945 GW844520, a novel anti-malarial mitochondrial electron transport inhibitor. *J Pharm Sci*
946 **95**, 2657-2672.
947 [124] Yeates CL *et al.* (2008). Synthesis and structure-activity relationships of 4-pyridones as
948 potential antimalarials. *J Med Chem* **51**, 2845-2852.
949 [125] Bueno JM *et al.* (2011). Potent antimalarial 4-pyridones with improved physico-chemical
950 properties. *Bioorg Med Chem Lett* **21**, 5214-8.
951 [126] Wernsdorfer WH and Payne D (1991). The dynamics of drug resistance in *Plasmodium*
952 *falciparum*. *Pharmacol Ther* **50**, 95-121.
953 [127] Winter RW *et al.* (2006). Evaluation and lead optimization of anti-malarial acridones. *Exp*
954 *Parasitol* **114**, 47-56.
955 [128] Chou AC and Fitch CD (1993). Control of heme polymerase by chloroquine and other
956 quinoline derivatives. *Biochem Biophys Res Commun* **195**, 422-7.
957 [129] Dorn A, Vippagunta SR, Matile H, Jaquet C, Vennerstrom JL and Ridley RG (1998). An
958 assessment of drug-haematin binding as a mechanism for inhibition of haematin
959 polymerisation by quinoline antimalarials. *Biochem Pharmacol* **55**, 727-36.

960 [130] Dorn A, Scovill JP, Ellis WY, Matile H, Ridley RG and Vennerstrom JL (2001). Short
961 report: Floxacrine analog WR 243251 inhibits hematin polymerization. *Am J Trop Med*
962 *Hyg* **65**, 19-20.
963 [131] Auparakkitanon S, Noonpakdee W, Ralph RK, Denny WA and Wilairat P (2003).
964 Antimalarial 9-anilinoacridine compounds directed at hematin. *Antimicrob Agents*
965 *Chemother* **47**, 3708-12.
966 [132] Auparakkitanon S, Chapoomram S, Kuaha K, Chirachariyavej T and Wilairat P (2006).
967 Targeting of hematin by the antimalarial pyronaridine. *Antimicrob Agents Chemother* **50**,
968 2197-200.
969 [133] Suswam E, Kyle D and Lang-Unnasch N (2001). *Plasmodium falciparum*: The effects of
970 atovaquone resistance on respiration. *Exp Parasitol* **98**, 180-7.
971 [134] Stocks PA, Barton V, Antoine T, Biagini GA, Ward SA and O'Neill PM (2014). Novel
972 inhibitors of the *Plasmodium falciparum* electron transport chain. *Parasitology* **141**, 50-
973 65.
974 [135] Winter RW, Kelly JX, Smilkstein MJ, Dodean R, Hinrichs D and Riscoe MK (2008).
975 Antimalarial quinolones: Synthesis, potency, and mechanistic studies. *Exp Parasitol* **118**,
976 487-497.
977 [136] Nilsen A et al. (2013). Quinolone-3-Diarylethers: A new class of antimalarial drug. Sci
978 Transl Med **5**, 177ra37.
979 [137] Salzer W, Timmler H and Andersag H (1948). Über einen neuen, gegen vogelmalaria
980 wirksamen verbindungstypus. *Chemische Berichte* **81**, 12-19.
981 [138] Fang J and Beattie DS (2003). External alternative NADH dehydrogenase of
982 *Saccharomyces cerevisiae*: A potential source of superoxide. *Free Radic Biol Med* **34**, 478-
983 488.
984 [139] Lane KD, Mu J, Lu J, Windle ST, Liu A, Sun PD and Wellems TE (2018). Selection of
985 *Plasmodium falciparum* cytochrome B mutants by putative PfNDH2 inhibitors. *Proc Natl*
986 *Acad Sci U S A* **115**, 6288-6290.
987 [140] Frueh L *et al* (2017). Alkoxycarbonate ester prodrugs of preclinical drug candidate ELQ-
988 300 for prophylaxis and treatment of malaria. *ACS Infect Dis* **3**, 728-735.
989 [141] Smilkstein MJ *et al.* (2019). ELQ-331 as a prototype for extremely durable
990 chemoprotection against malaria. *Malar J* **18**, 291.

[142] da Cruz FP *et al.* (2012). Drug screen targeted at *Plasmodium* liver stages identifies a potent multistage antimalarial drug. *J Infect Dis* **205**, 1278-1286.

[143] Cowley R *et al.* (2012). The development of quinolone esters as novel antimalarial agents targeting the *Plasmodium falciparum* bc_1 protein complex. *Med Chem Comm* **3**, 39.

[144] Sievers F *et al.* (2011). Fast, scalable generation of high-quality protein multiple sequence alignments using Clustal Omega. *Mol Syst Biol* **7**, 539-545

[145] Sobolev V, Sorokine A, Prilusky J, Abola EE and Edelman M (1999). Automated analysis of interatomic contacts in proteins. *Bioinformatics* **15**, 327-332.

Figure Legends

Figure 1

Cartoon representation of the atomic structure of cyt *b* (green) and the ISP (orange) of yeast cyt bc_1 (1EZV.PDB, [39]) with stigmatellin (Stg, pink) bound at Q_o. The ISP [2Fe2S] cluster, cyt *b* haems (red)- and sidechains of interest as discussed in the text are represented in wireframe form.

Figure 2

Schematic sketch of the electron- and proton transfer pathways of the cyt bc_1 Q-cycle. Cyt *b* is represented in light grey, with the Q_o/Q_i-pockets in dark grey. 'Red' and 'ox' refer to the reduced and oxidised states of the various redox carriers. The positive and negative sides of the energised inner mitochondrial membrane are indicated accordingly.

Figure 3

Cartoon of the secondary structure and membrane disposition of cyt *b*, displaying the location of Q_o (red) and Q_i (blue) residues of interest (*S. cerevisiae* notation) as discussed in the text. Transmembrane- and surface helices are identified in upper and lower case, respectively. 'n' and 'p' refer to the negative and positive sides of the energised inner mitochondrial membrane.

Figure 4

Structures of selected anti-malarial compounds in use and under development discussed in the text.

Figure 5

Protein sequence alignment of the Q_i-site region of cytochrome *b* from *P. falciparum* (Pf, UniProtKB accession: Q02768), *S. cerevisiae* (Sc, P00163), *Gallus gallus* (chicken, Gg, P18946), *Homo sapiens* (Hs, P00156) and *Bos taurus* (cow, Bt, PB00157). Sequence conservation in the aligned sequences is indicated using the Clustal Omega convention [144], with asterisks, colons and periods indicating complete conservation, conservative substitutions and semi-conservative substitutions, respectively. Sequence data were obtained from the UniProt database. Arrows underneath the alignment indicate α-helices as identified in Fig. 3. Residues in the bovine cytochrome *b* atomic structures 1NTK [35], 4D6T [5] and 4D6U (*ibid*) in potential hydrogen-bonding association with bound antimycin, and the 4(1H)-pyridones GW844520 and GSK932121 are indicated by red, blue and green circles, respectively. Residues forming stabilising hydrophobic contacts with bound GW844520 in the bovine 4D6T structure are shaded in yellow. (GSK932121 displays similar binding interactions). Protein-ligand associations indicated in this figure were predicted- and analysed using the LPC software package [145].

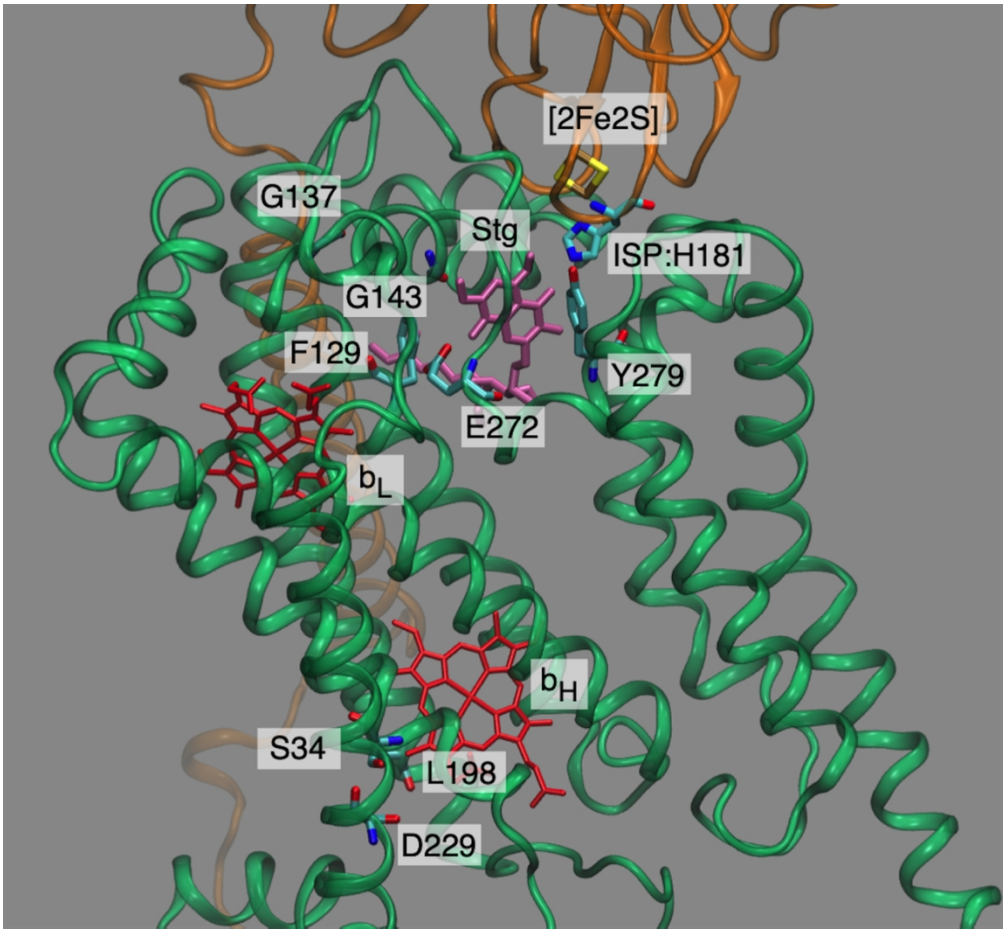

Figure 1 / Cartoon representation of the atomic structure of cyt b (green) and the ISP (orange) of yeast cyt bc1 (1EZV.PDB [39]) with stigmatellin (SMA, pink) bound at Qo. The ISP [2Fe2S] cluster, cyt b haems (red)- and sidechains of interest as discussed in the text are represented in wireframe form.

109x101mm (300 x 300 DPI)

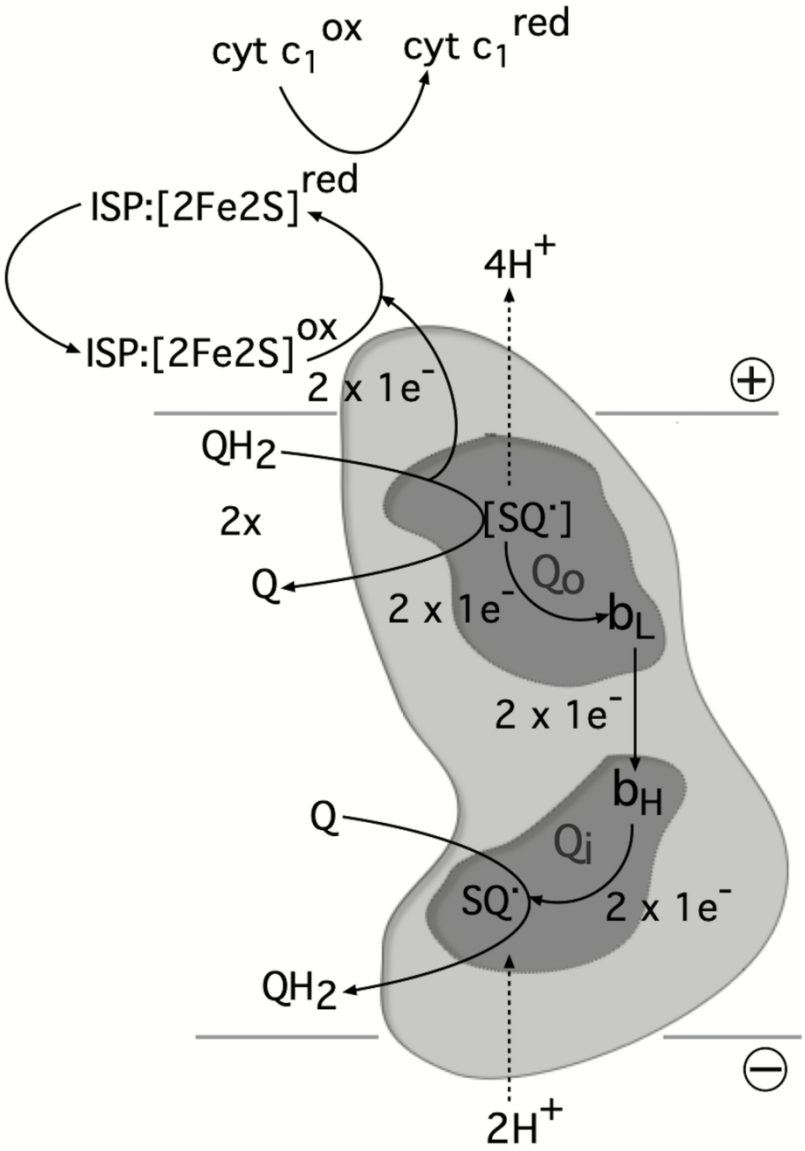

Figure 2 / Schematic sketch of the electron- and proton transfer pathways of the cyt bc1 Q-cycle. Cyt b is represented in light grey, with the Qo/Qi-pockets in dark grey. 'Red' and 'ox' refer to the reduced and oxidised states of the various redox carriers. The positive and negative sides of the energised inner mitochondrial membrane are indicated accordingly.

102x129mm (300 x 300 DPI)

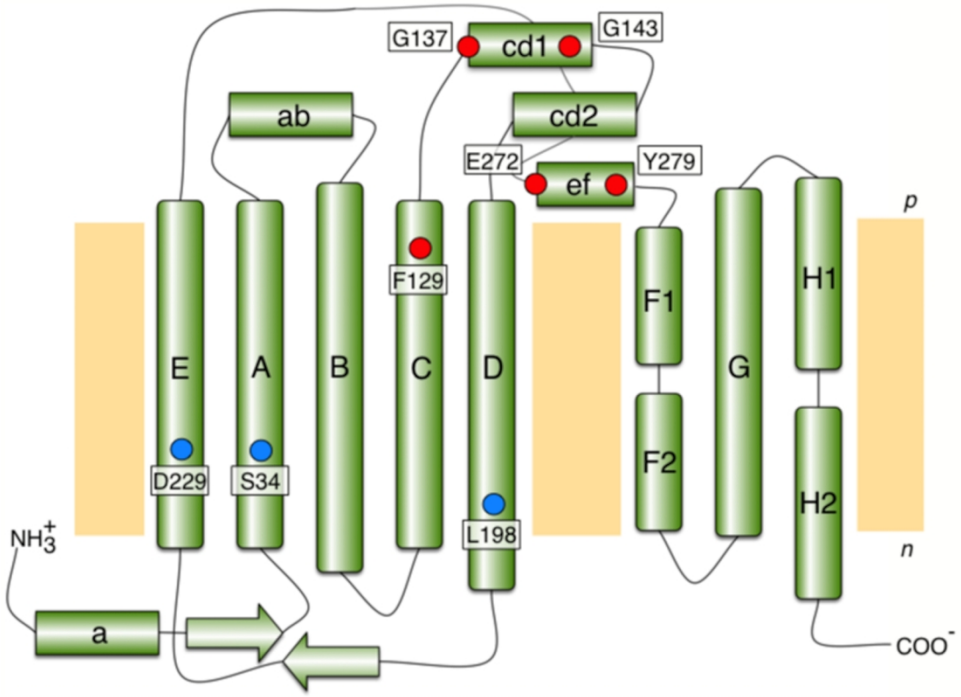

Figure 3 / Cartoon of the secondary structure and membrane disposition of cyt b, displaying the location of Qo (red) and Qi (blue) residues of interest (S. cerevisiae notation) as discussed in the text. Transmembrane- and surface helices are identified in upper and lower case, respectively. 'n' and 'p' refer to the negative and positive sides of the energised inner mitochondrial membrane.

139x106mm (300 x 300 DPI)

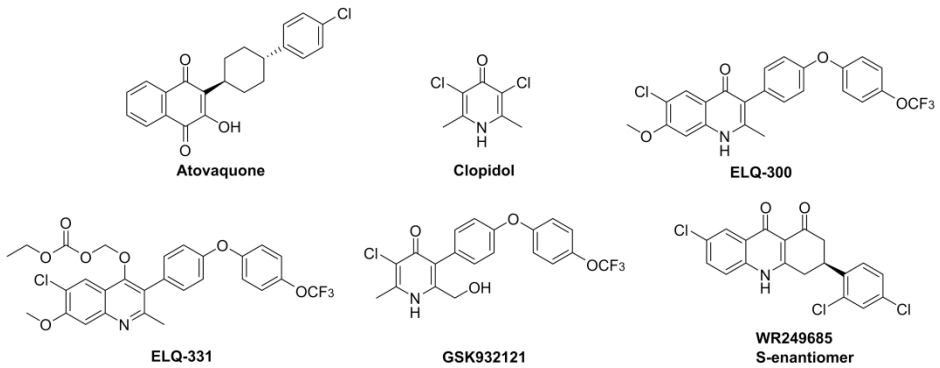

Figure 4 / Structures of selected anti-malarial compounds in use- and under development as discussed in the text.

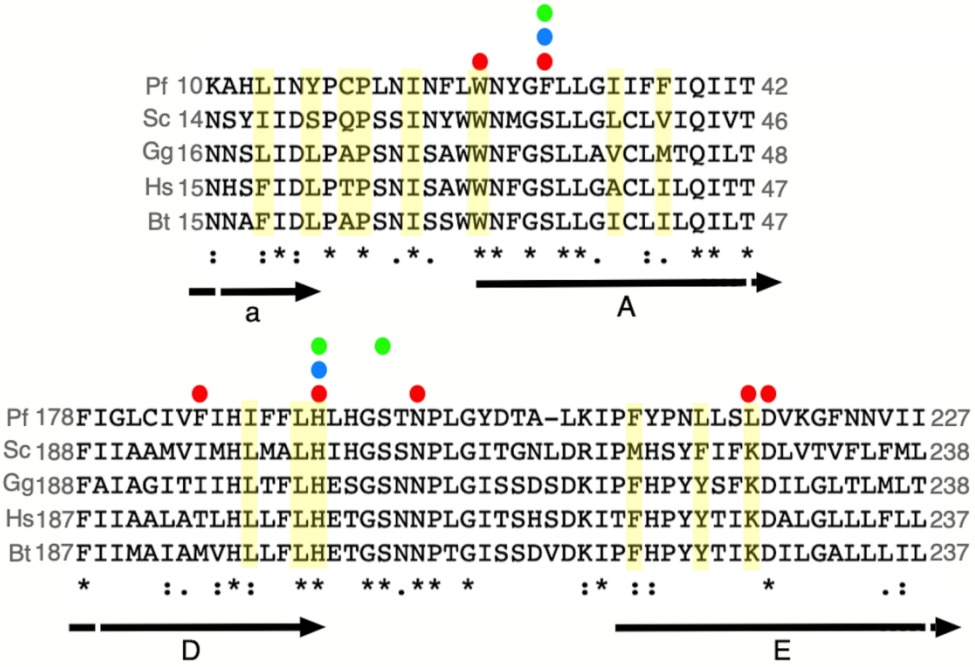

Figure 5 / Protein sequence alignment of the Qi-site region of cytochrome b from P. falciparum (Pf, UniProtKB accession: Q02768), S. cerevisiae (Sc, P00163), Gallus gallus (chicken, Gg, P18946), Homo sapiens (Hs, P00156) and Bos taurus (cow, Bt, PB00157). Sequence conservation in the aligned sequence data is indicated using the Clustal Omega convention [144] , with asterisks, colons and periods indictating complete conservation, conservative substitutions and semi-conservative substitutions respectively. Sequence data were obtained from the UniProt database. Arrows underneath the alignment indicate α-helices as identified in Fig. 3. Residues in the bovine cytochrome b atomic structures 1NTK [35], 4D6T [5] and 4D6U (ibid) in potential hydrogen-bonding association with bound antimycin, and the 4(1H)-pyridones GW844520 and GSK932121 are indicated by red, blue and green circles respectively. Residues forming stabilising hydrophobic contacts with bound GW844520 in the bovine 4D6T structure are shaded in yellow. (GSK932121 displays similar binding interactions). Protein-ligand associations indicated in this figure were predicted- and analysed using the LPC software package [145].

149x104mm (300 x 300 DPI)